ANTHROPOMORPHIC VASE - AG ALLOY - ROMAN TIMES

Artefact name Anthropomorphic vase

Authors (HE-Arc CR, Neuchâtel, Neuchâtel, Switzerland). (Christian Degrigny, None) & Solène. Béguelin (HE-Arc CR, Neuchâtel, Neuchâtel, Switzerland) & Valentin. Boissonnas (HE-Arc CR, Neuchâtel, Neuchâtel, Switzerland)

Url /artefacts/1447/

The object



Fig. 1: Front of the vase,

Credit HE-Arc CR_S.Béguelin.

Description and visual observation

This work is licensed under CC BY-NC-ND 4.0

Description of the artefact	This archaeological anthropomorphic vase has a round body topped by a woman's face. At the top of the handle is a ram's head. The object is covered with a brown-grey corrosion layer. The metal surface is deformed on the face and the body. H =15.5cm ; Ø = 26cm.
Type of artefact	Vessel
Origin	Unknown
Recovering date	Date unknown
Chronology category	Roman Times
chronology tpq	----
chronology taq	----
Chronology comment	
Burial conditions / environment	Soil
Artefact location	Musée d'Art et d'Histoire de la Neuveville, La Neuveville, Bern
Owner	Musée d'Art et d'Histoire de la Neuveville, La Neuveville, Bern
Inv. number	MHLN-2006-24.076
Recorded conservation data	A conservation-restoration treatment was carried out in 2023. The object underwent mechanical and chemical treatment (alkaline dithionite baths).

Complementary information

The object was donated to the museum without any information about its provenance or possible dating.

Study area(s)



Fig. 2: Locations of the four points analysed with X-ray fluorescence (black arrows A-D), the four samples (numbers 1-4) and the cross-section (yellow) analysed with SEM-EDS,

Credit HE-Arc CR_S.Béguelin.

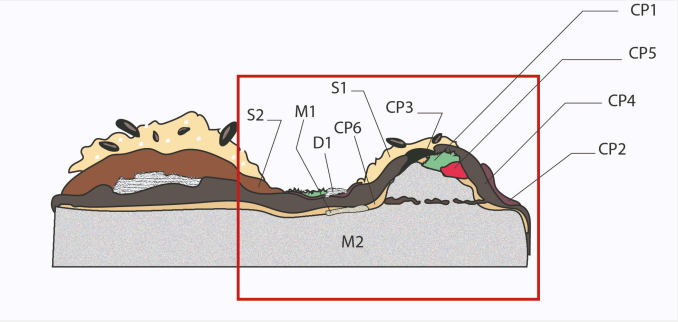
Binocular observation and representation of the corrosion structure

The schematic representation below gives an overview of the corrosion structure encountered on the object from a first visual macroscopic observation.

This work is licensed under CC BY-NC-ND 4.0

Strata	Type of Stratum	Principal Characteristics
S1	Soil (with mica / feldspath)	light beige, medium, non-compact, powdery and containing black-brown scattered aggregates
S2	Soil	brown, medium, compact, very soft
D1	Deposit	white, thin, compact, hard, brittle
CP1	Corroded product	light green, thin, discontinuous, non-compact, powdery
CP2	Corroded product	pinkish brown, thin, discontinous, compact, soft
CP3	Corroded product	black, medium, discontinous, compact, hard
CP4	Corroded product	dark brown, medium, continous, compact, soft
CP5	Corroded product	red, thin, discontinous, non-compact, powdery, soft
CP6	Corroded product	light beige, thin, continous, compact, very soft
M1	Metal	yellowish grey, metallic, hard
M2	Metal	grey-white, metallic, soft

Table 1: Description of the principal characteristics of the strata as observed under binocular.



Credit HE-Arc CR_S.Béguelin.

Fig. 3: Stratigraphic representation of the corrosion structure of the vase by macroscopic and binocular observation with indication of the corrosion structure used to build the MiCorr stratigraphy of Fig. 4 (red rectangle),

MiCorr stratigraphy(ies) – Bi

This work is licensed under CC BY-NC-ND 4.0

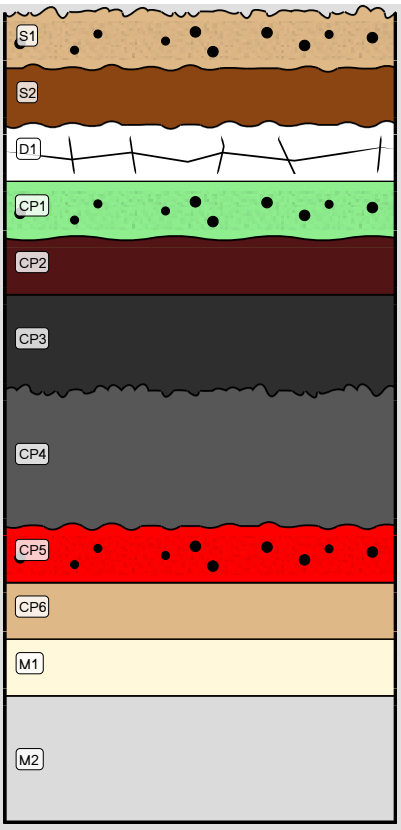
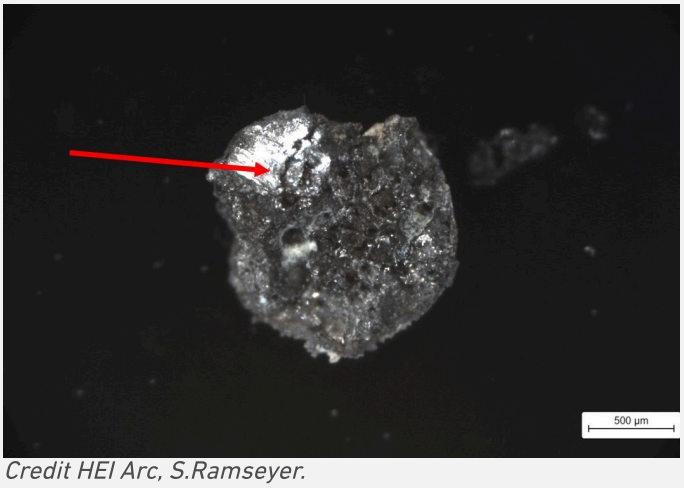


Fig. 4: Stratigraphic representation of the corrosion structure of the vase observed macroscopically under binocular microscope using the MiCorr application with reference to Fig. 3. The characteristics of the strata are only accessible by clicking on the drawing that redirects you to the search tool by stratigraphy representation, credit HE-Arc CR, S.Béguelin.

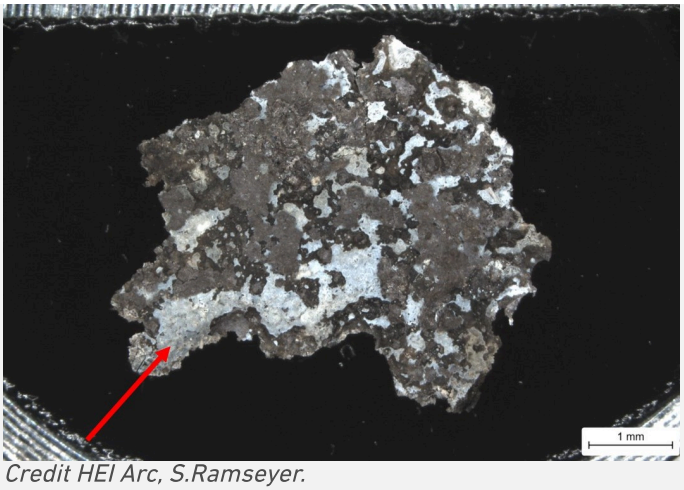
Sample(s)



Credit HEI Arc, S.Ramseyer.

Fig. 5: Micrograph of sample 1 (Fig. 2) of the vase showing a blister (the red arrow corresponds to the area where EDX analysis was carried out),

This work is licensed under CC BY-NC-ND 4.0



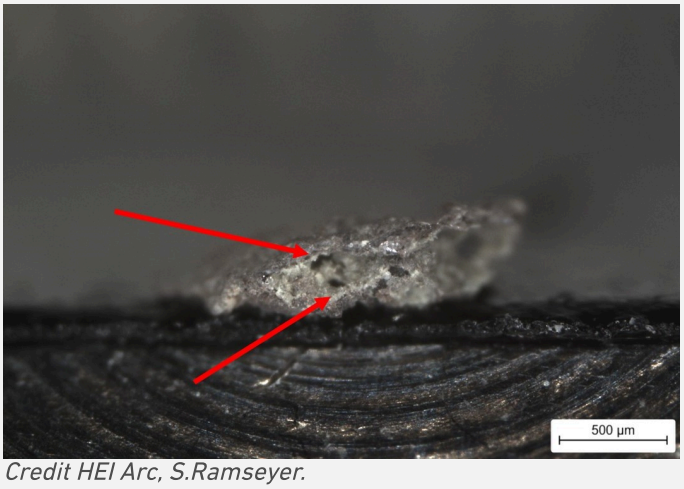
Credit HEI Arc, S.Ramseyer.

Fig. 6: Micrograph of sample 2 (Fig. 2) of the vase showing a concretion (the red arrow corresponds to the area where EDX analysis was carried out),



Credit HEI Arc, S.Ramseyer.

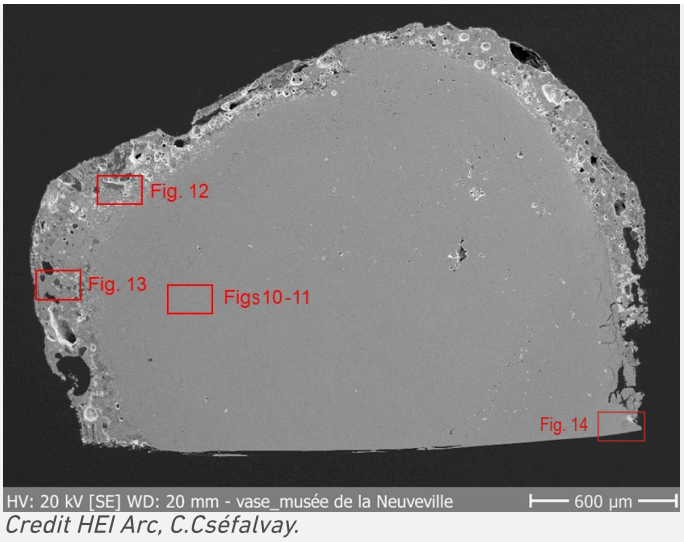
Fig. 7: Micrograph of sample 3 (Fig. 2) of the vase showing a small black element (the red arrow corresponds to the area where EDX analysis was carried out),



Credit HEI Arc, S.Ramseyer.

Fig. 8: Micrograph of sample 4 (Fig. 2) of the vase showing a piece of mineralized metal (the red arrows correspond to the areas where EDX analyses were carried out),

This work is licensed under CC BY-NC-ND 4.0



Credit HEI Arc, C.Cséfalvay.

Fig. 9: SEM picture (SE mode) of the cross-section of the vase showing the location of Figs.10 to 14, unetched,

Description of sample	Samples 1-4 were taken from different areas of the object (Fig. 2) using a scalpel; they were not embedded. The cross-section embedded corresponds to a transversal cut made on the foot of the container (Fig. 2). A metallic core is present below the corrosion layers (Fig. 9).
Alloy	Ag alloy
Technology	Annealed after cold working
Lab number of sample	None.
Sample location	Musée d'Art et d'Historie de la Neuveville, La Neuveville, Bern
Responsible institution	Musée d'Art et d'Historie de la Neuveville, La Neuveville, Bern
Date and aim of sampling	20. of March 2023. For analysis and information purposes with a view to conservation-restoration treatment

Complementary information

None.

Analyses and results

Analyses performed:

Non-invasive approach

- XRF with handheld portable X-ray fluorescence spectrometer (NITON XL3t 950 Air GOLDD+, Thermo Fischer®). General Metals mode, acquisition time 60s.

Invasive approach

- Optical microscopy: the sample is embedded in an EpoFix resin and polished, then it is observed on a digital microscope KEYENCE VHX-7000 in bright field.

- SEM-EDS: the sample is coated with a carbon layer and analyses are performed on a SEM-EDX JEOL JSM-7500 TFE equipped with a silicon-drift EDS Oxford detector. Accelerating voltage is 20 kV and probe current from a 1 to 10nA.

- Metallography: the polished sample (polishing conditions: final polishing disc made of short-haired synthetic felt and oil in aqueous emulsion (Lubricant DP, red)) is etched in an oxygenated ammoniacal solution (30 ml NH_4OH + 10ml H_2O_2 then add H_2O_2 until a reaction occurs). Two attempts were made: the first with just the oxygenated ammoniacal solution and the second by putting the same solution on the polishing disc instead of the lubricant

This work is licensed under CC BY-NC-ND 4.0

(mechanical and chemical action). The second attempt worked best. The sample was then observed by optical microscopy in bright field.

Non invasive analysis

The XRF analysis of the vase was carried out before sampling on four areas (Fig. 2). During the analysis, the layers of soil, corrosion and metal are analysed at the same time. The metal is probably a silver alloy with a small amount of Cu (and possibly Bi?). Some of the other elements detected are part of the burial environment (Al, Si, Fe, Cr) and corrosion products (Br, Cl). Titanium is probably an artefact.

Elements (wt %)	Ag	Bi	Cu	Cr	Sn	Pb	Zn	Br	Cl	Al	Fe	V	Ti	Si
A	80	2	2	1	1	<0.5	-	++	+	7	2	-	<0.5	6
B	93	1	-	<0.5	2	-	-	+	<	-	2	-	-	-
C	75	2	1	1	1	<0.5	<0.5	++	++	13	2	-	-	5
D	78	2	2	1	-	<0.5	<0.5	++	+	9	3	<0.5	<0.5	5

Table 2: Chemical composition of the surface of the vase at four points shown in Fig. 2. The results are rounded up to the nearest whole number. Method of analysis: handheld portable X-ray fluorescence spectrometer, HE-Arc CR.

Metal

The analysis of the metal was done with EDX.

The base metal consists of 1.5% copper, 1.8% zinc and 96.7% silver by weight. Silver is therefore only lightly alloyed. The zinc and copper are in the form of inclusions (Figs. 10 and 11). The grains are clearly visible, copper and zinc have precipitated in the grain boundaries and develop intergranular corrosion (Fig. 13). Iron inclusions are also visible in places (Fig. 12). The presence of bromine and chlorine has been attested (Fig. 13).

As a result of the chemical attack, various structures are visible. We can see twin lines (Fig. 14), which means that the structure has been several times annealed after hammering. We can also see in some places the presence of strain lines, which characterise the final hammering of a structure without annealing (Scott, 1991).

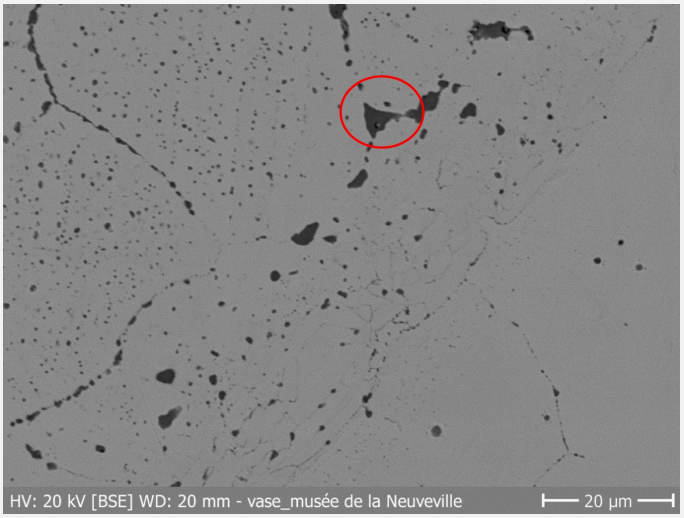
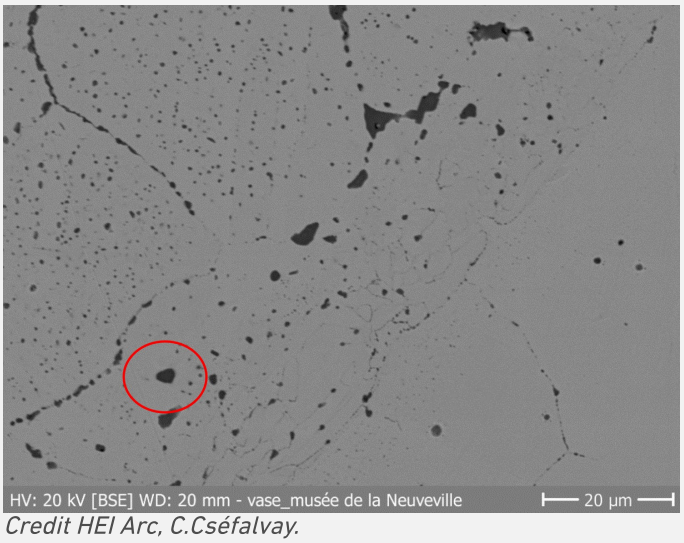


Fig. 10: SEM picture (BSE mode) of the metal sample from Fig. 9 (detail), with zinc inclusion,

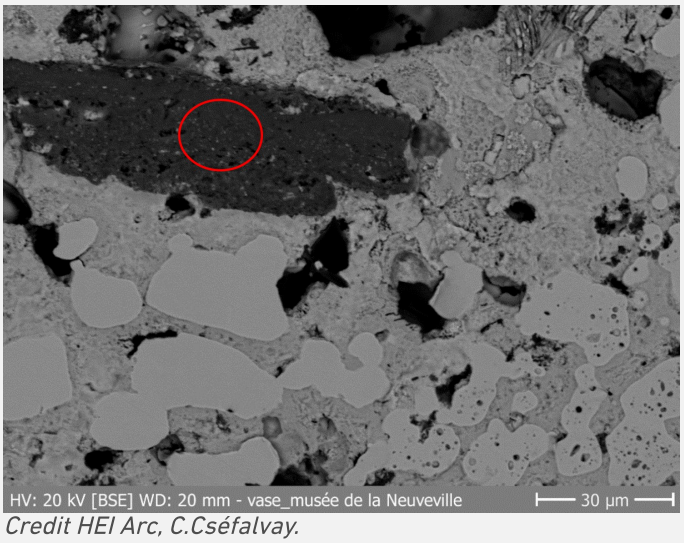
This work is licensed under CC BY-NC-ND 4.0

Credit HEI Arc, C.Cséfalvay.



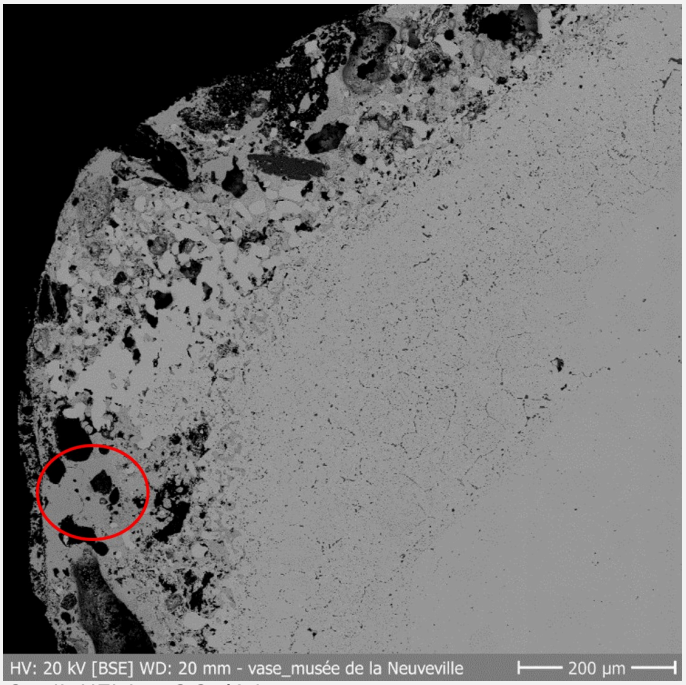
Credit HEI Arc, C.Cséfalvay.

Fig. 11: SEM picture (BSE mode) of the metal sample from Fig. 9 (detail), with copper inclusion,



Credit HEI Arc, C.Cséfalvay.

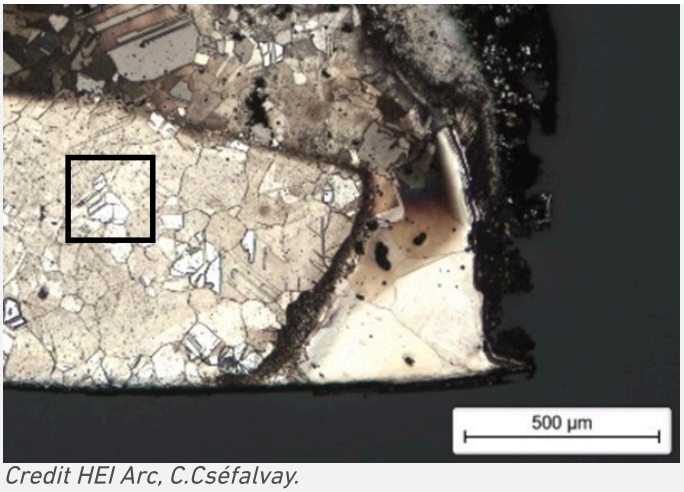
Fig. 12: SEM picture (BSE mode) of the metal sample from Fig. 9 (detail), with iron inclusion,



Credit HEI Arc, C.Cséfalvay.

Fig. 13: SEM picture (BSE mode) of the metal sample from Fig. 9 (detail) with high amount of silver, bromine and chlorine in the red circle,

This work is licensed under CC BY-NC-ND 4.0



Credit HEI Arc, C.Cséfalvay.

Fig.14 : Micrograph of the sample after etching. Twin lines are clearly visible in the black square,

Microstructure	Large and small polygonal grains with few twins + strain lines
First metal element	Ag
Other metal elements	Cu, Zn

Complementary information

None.

Corrosion layers

Observation of the cross-section under a microscope does not clearly distinguish the different corrosion layers on the vase. We can see a continuous, dark brown corrosion layer. The area where the sample was taken does not contain any light green or red corrosion. On the other hand, we can see that the silver forms a sort of blister which makes it difficult to distinguish the limit of the original surface (Fig. 15).

Mapping using SEM-EDS shows that the corrosion layer consists mainly of silver, bromine and chlorine, with a larger amount of chlorine next to the metal surface (CP2 in Fig. 16). There are also inclusions of calcium, iron, chromium and lead combined with oxygen. Secondly, we can see the formation of intergranular corrosion with the presence of copper and zinc at the grain boundaries (Figs. 16 to 17).

Raman analysis was carried out on a sample of mineralised metal (Fig. 18). The spectrum obtained does not correspond to those presented in the literature for silver chloride. Therefore, it remains a hypothesis.

Based on the elemental chemical distribution, we can interpret better the EDX results of samples from Figs. 5 to 8. Indeed, blisters (Fig. 5) consist mainly of silver polluted on its surface with bromine and chlorine (Fig. 17). As for the piece of mineralised metal (Fig. 8), it also consists largely of silver, bromine and chlorine (same corrosion products as the blister). This is rather typical for such an archaeological object recovered from the ground (Marchand et al., 2014). The concretion (Fig. 6) is made up of carbon, oxygen, sodium, silicon, aluminium, calcium, a little potassium and phosphorus, also from the burial context. The black element (Fig. 7) could be likened to mica or feldspath (Figs. 16 and 17 with detail in Fig. 12). There is magnesium, silicon and oxygen, again from the environment in which the object was buried.

This work is licensed under CC BY-NC-ND 4.0

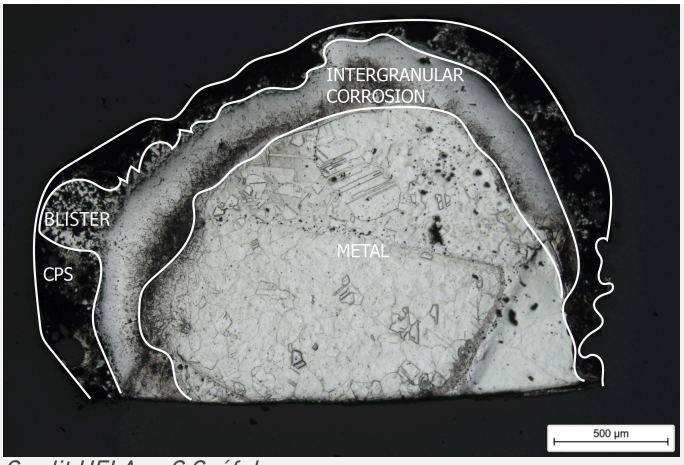


Fig. 15: Micrograph of the corrosion structure from Fig. 9 with the subdivision of the different strata,

Credit HEI Arc, C.Cséfalvay.

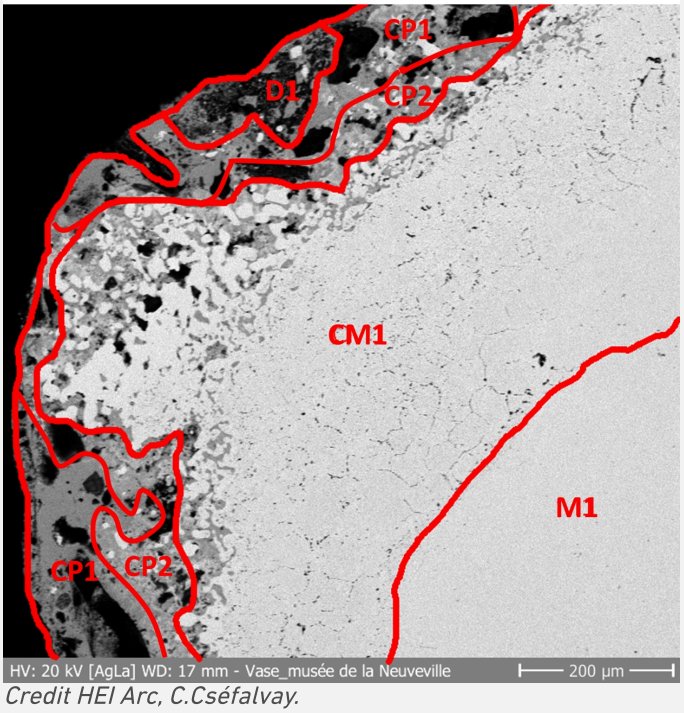


Fig. 16: Elemental distribution of Ag within the corrosion structure from Fig. 15 (detail) with the subdivision of the different strata,

Credit HEI Arc, C.Cséfalvay.

This work is licensed under CC BY-NC-ND 4.0

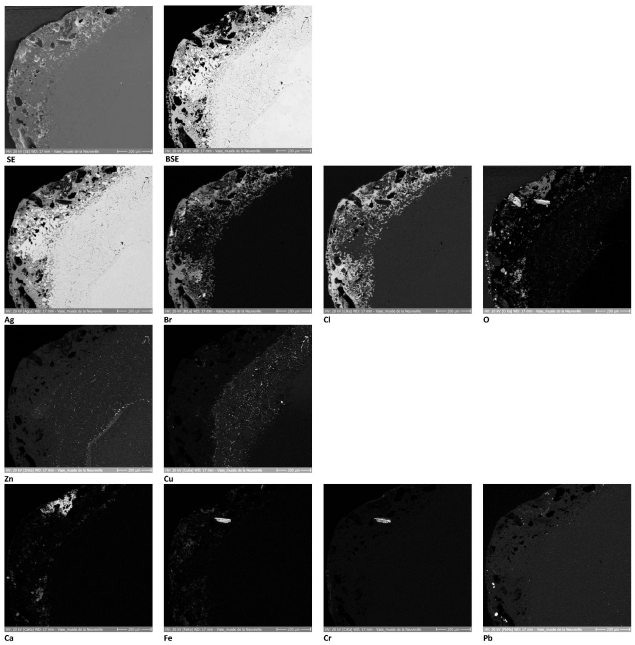


Fig. 17: SEM picture (BSE-mode) similar to Fig. 16 (detail of Fig. 15) and elemental chemical distribution,

Credit HEI Arc, C.Cséfalvay.

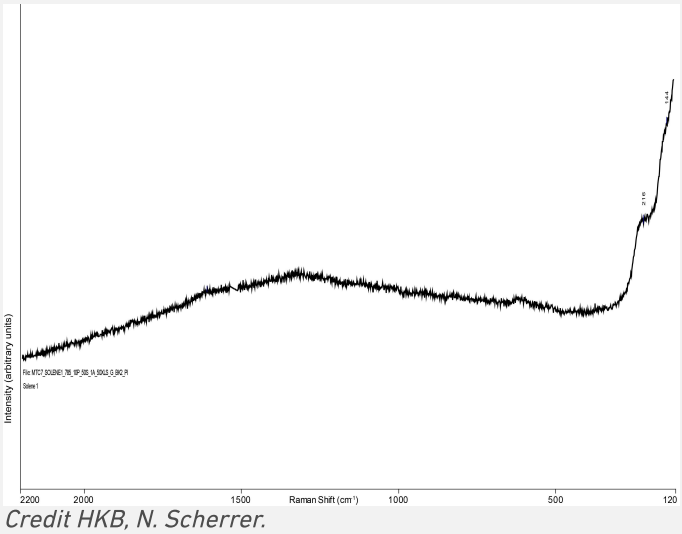


Fig. 18: Raman spectrum of the mineralised metal sample (Fig. 8) possibly silver chloride,

Credit HKB, N. Scherrer.

Corrosion form	Uniform - intergranular
Corrosion type	Silver corrosion

Complementary information

None.

MiCorr stratigraphy(ies) – CS

This work is licensed under CC BY-NC-ND 4.0

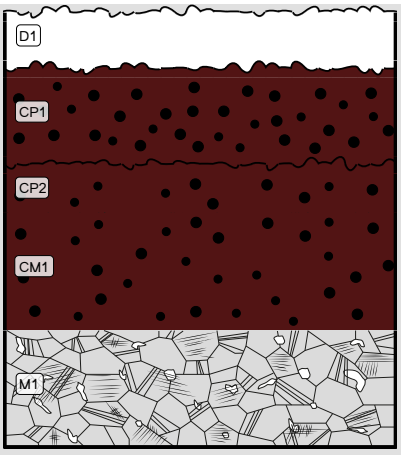
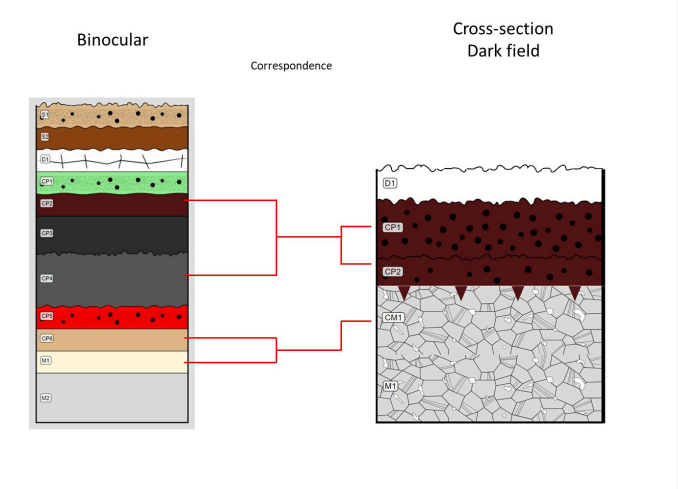


Fig. 19: Stratigraphic representation of the sample of the vase observed in cross-section under dark field using the MiCorr application. The characteristics of the strata are only accessible by clicking on the drawing that redirects you to the search tool by stratigraphy representation. This representation was build according to Fig.15, credit HE-Arc CR, S.Béguelin.

Synthesis of the binocular / cross-section examination of the corrosion structure

Compared with Figure 4, the amount of information is just limited to an area where there is only one blister. Observation of the cross-section did not reveal all the corrosion layers visible on the entire object when it was probed under binoculars. In fact, only two layers of corrosion are visible (CP1 and CP2) (Fig. 19). They correspond to two different corrosion layers of the Bi MiCorr stratigraphy (CP2 and CP4, Fig. 4). CM1 (Fig.19) could correspond to CP6 and M1 on Fig. 4. M2 on Fig. 4 corresponds to M1 on Fig. 19.

The lack of information when examining the cross-section is due to the fact that the colours of the layers are very close to each other. The sample is fairly representative of the object, showing mainly a layer of corrosion rich in Ag, Cl and Br on a metal that is subject to intergranular corrosion. The sample's location was chosen because it's a discrete area and it allowed us to analyse the metal at its core.



Credit HE-Arc CR_S.Béguelin.

Fig. 20: Stratigraphic representation side by side of binocular view and cross-section (dark field),

Conclusion

The base metal of this anthromorphic vase is low-alloy silver with 1.5% copper, 1.8% zinc by weight. Copper and zinc inclusions have precipitated at the grain boundaries, forming intergranular corrosion below the corrosion laysers. Differences in electrochemical activity of elements (Zn versus to Ag) lead to localised corrosion which developed as intergranular corrosion (Liu et al., 2020).

In terms of the microstructure, twin lines can be observed, which means that several annealing and hammering processes were carried out successively. In some places, strained lines can be seen, which characterise the cold hammering of a structure that has been hammered and annealed (Scott, 1991).

This work is licensed under CC BY-NC-ND 4.0

The sediments and corrosion products present on the object are due to the environment in which it was buried. According to the analyses carried out (X-ray fluorescence and scanning electron microscopy coupled to the EDS system), the sediments consist mainly of silicon, calcium and aluminium. The corrosion products of silver are mainly chlorides and bromides.

In a buried environment, silver can corrode strongly under the effect of relative humidity and soluble salts. Chloride ions are particularly corrosive to silver. Silver then reacts with the chlorides to form silver chloride (horned silver) (Marchand et al., 2014). The basic colour of silver chloride is white, but when polluted by other elements, it can become grey, brown or dull lavender (Selwyn, 2004). Dissolved bromide ions come from the decomposition of organic matter, and silver can also react with them to form silver bromide (Selwyn, 2004). The mineralisation process occurs slowly and this state allows the traces left by tools and decorations on the object to be preserved (Costa, 2001). In some cases, such as the vase, the metal is only mineralised in places.

The limit of the original surface (limitos) could not be located precisely but it certainly within the silver-based corrosion products.

References

References on analytical methods and interpretation

1. Scott, D. (1991) Metallography and Microstructure of Ancient and Historic Metals. Los Angeles, Getty Conservation Institute.
2. Selwyn, L. (2004) Métaux et corrosion : un manuel pour le professionnel de la conservation. Ottawa, Institut canadien de conservation.
3. Costa, V. (2001) The deterioration of silver alloys and some aspects of their conservation. Studies in Conservation, vol. 46, 18-34.
4. Liu et al. (2020) Scanning electrochemical cell microscopy: A powerful method to study the intergranular corrosions of archaeological silver artifacts. Journal of Cultural Heritage, no. 46, 176-183.

Reference on object and sample

5. Marchand et al. (2014) Degradation of archaeological horn silver artefacts in burials. Heritage Science, vol 2, 1-7.

This work is licensed under CC BY-NC-ND 4.0